The 6th Saudi Engineering Conference, KFUPM, Dhahran, December 2002 Vol. 5. 313

FATIGUE DAMAGE IN WOVEN CARBON FABRIC/EPOXY LAMINATES AT NON-AMBIENT TEMPERATURES

Z. Khan, [1], R. Khan, [2], F. Al-Sulaiman [1], and N. Merah [1]

1. Associate Professor, Mechanical Engineering Department, KFUPM, Dhahran, Saudi Arabia
2.Former Graduate Student, KFUPM, Dhahran, Saudi Arabia
E-mail: zukhan@kfupm.edu.sa

ABSTRACT

The mechanisms involved in initiation and development of non-ambient temperature fatigue damage in Plain Weave-Woven Carbon fabric/epoxy Composite laminates is explored. Laminates obtained from prepreg woven carbon fabric layers were subjected to tension-tension cyclic loading at –20^{o}C, 0^{o}C, 24^{o}C 100^{o}C and 150^{o}C. Two different stacking sequences, a unidirectional $[0]_8$, and an angle plied $[0,0,45,-45]_s$ sequence were studied. Optical microscopy, enhanced-dye penetrant X-ray radiography, and scanning electron fractography were employed to examine the fatigue damage mechanisms operative at various temperatures. Temperature was found to have a significant effect on the fiber/matrix bonding and interply delamination characteristics of these woven carbon fabric/epoxy laminates.

Keywords: *Fatigue, composites, damage mechanisms, woven fabric, tension-tension loading, non-ambient temperature*

المخاص

إجريت هذه الدراسة لتشخيص الآليات المسؤولة عن الضرر الكلي الملحوظ في الصفائح المنسوجة من مركب الكربون واللصاق (Epoxy). تتكون هذه الصفائح من ثمان طيات مصنوعة من الكربون المشّرب . أجريت تجارب الإجهاد الدوري (مـ د - مد) على المركب تحت الدرجات الحرارية المئوية الآتية – ٢٠ ، ٠ ، ٢٤ ، ١٠٠ و ١٥٠ .
أختير للدراسة صفائح مكدسة في الإتجاه الأحادي وصفائح في اتجاهات أخرى .

استعمل الصباغ المقوى المتغلغل مع المجهر البصري والماسح الألكتروني SEM لتشخيص الآليات المسؤولة عن الضرر . يستخلص من هذه الدراسة أن درجة الحرارة تؤثر كثيرا على قوة ترابط الياف المركب وعلى قوى المادة الرابطة بين الطيات.

1. INTRODUCTION

Due to their increasing use under cyclic loading conditions, fatigue studies in Carbon Fiber Reinforced Plastics (CFRPs) have been a focus of considerable attention in recent decades. Under cyclic loading these materials exhibit extremely complex sequential damage accumulation process involving several micro-damage events such as transverse matrix cracking, ply delamination, fiber matrix debonding, and fiber fracture. During the past two decades investigators have employed various techniques such as scanning electron microscopy, x-ray radiography, edge replication, acoustic emissions, and C-scan acoustics to investigate fatigue damage initiation and damage progression processes. Notable among these investigations are the study aimed at detection of delamination cracks in carbon fabric-reinforced composite [Todoroki,1994], investigation of progressive fatigue damage in plain-weave glass fabric reinforced plastics [Kim,1997, Tkemura, 1994], use of ultrasonic C-scan to determine the ply stacking sequence and delamination in Carbon Fiber-reinforced Composites [Smith,1994], and fatigue damage evolution and development in Carbon Fiber-reinforced PEEK Composite specimens in 3-point bending fatigue [Dillon, 1995]. In other notable studies [Takeda,1998] micro-grid method was used to measure the displacements in 90^o ply Carbon Fiber-reinforced cross ply laminates with transverse cracks or both transverse cracks and delamination. Recently fatigue damage in woven Carbon Fiber-reinforced plastics have been explored [Gilchrist,1998] and [Khan,1998]. Gilchrist determined the flexural fatigue response of woven laminates under three-point bending. Scanning Electron Microscope was used to characterize fatigue damage. Khan et al examined the fatigue damage mechanism in 8-ply plain-weave woven carbon fabric-reinforced polyester using scanning electron microscopy, edge replication, and x-ray radiography.

In addition to ambient condition applications, CFRPs are now rapidly becoming candidates for applications where elevated or cryogenic temperatures are also encountered. This increasing use of CFRPs under non-ambient temperature cyclic loading conditions is making it essential that the effect of temperature on the fatigue damage behavior of CFRPs should be properly investigated. Proper characterization of fatigue damage initiation and accumulation mechanisms is essential for development of reliable methodologies for life prediction in CFRPs subjected to non-ambient cyclic loading conditions.

To date only a hand full of studies have been undertaken to investigate damage accumulation under fatigue loading at non-ambient temperature conditions. Scanning electron microscopy and edge replication techniques were used to characterize flexural fatigue damage at elevated temperatures for satin woven carbon fiber-reinforced plastics [Miyano,1994 ,1997]. In another study the effects of test temperatures on damage accumulation behavior and modulus reduction of carbon fiber/epoxy cross ply laminates under cyclic and monotonic loading has been explored [Matsuhisa,1993]. Nakamura et al

Top

studied the influence of temperature on the growth from mesocracks to macrocracks at elevated temperatures in carbon/glass fiber reinforced /PEEK composites [Nakamura,1998].

The work presented here attempts to provide some more answers to the issue of accurate characterization of fatigue damage initiation and damage accumulation process in a plain-weave woven carbon fabric/epoxy composites subjected to non-ambient temperature cyclic loading.

2. MATERIAL AND SPECIMEN GEOMETRY

Epoxy-impregnated plain-weave woven carbon fabric layers having 60 vol % carbon fibers were used to obtain 300 mm X 300 mm, 8-ply panels. The panels were produced in an autoclave at a curing temperature of 177^o C and curing pressure of 8 bars. Two different fabric layer stacking sequences, the unidirectional $[0]_8$ (referred as class1) and the angle ply $[0,0,45,-45]_s$ (referred as class 2) were used. Fatigue test coupons were machined from these panels. A ±100 kN Instron 8501 material testing system was used for fatigue testing. All fatigue tests were carried out under load control using an R ratio ($R= \sigma_{min}/\sigma_{max}$) of 0.1 and a frequency of 20 Hz. During the fatigue loading one edge was continuously examined with the help of an industrial video camera, while the other edge was monitored through an optical microscope providing a 300x view of the edge. A 35 mm camera attached to the microscope captured the edge damage at regular intervals.

Non-ambient temperature fatigue tests were carried out by enclosing the specimens in Plexiglas chambers. For elevated temperature testing, electrical heating tapes, lined around the inner walls of one chamber, acted as the uniform source of heat. Testing at sub-room temperature was carried out by circulating a refrigerant (a solution of 60% methanol-40% water) through copper tubes in the second chamber. Adhesively taped thermocouples on the specimen surface enabled continuous monitoring of test temperature throughout the test. A temperature controller maintained the temperature within ± 1^o C of the desired test temperature.

Enhanced dye x-ray radiography was performed on the fatigued specimens to examine the internal damage. A special Zinc Iodide solution having the composition of 60 gm Zinc Iodide (ZnI_2), 8 ml Water (H_2O), 10 ml Isopropyl Alcohol and 3 ml Kodak Photoflo-200 was used for radiography contrast enhancement A hypodermic syringe was used to inject the dye at the edges of the coupons and in the visible damaged sites. A Seimens Polyphos-30 X-ray machine was used for this x-ray radiography at 40 kV with a rate of 0.2 mA/sec.

3. GENERALIZED FATIGUE BEHAVIOR

The results of all fatigue tests carried out at various temperatures are graphically displayed in the form of S-N curves in figure 1 and 2. It is evident from these figures that for both classes of the laminates, test temperatures have a pronounced influence on their fatigue resistance. When compared to room temperature, the fatigue life is significantly increased at lower temperatures (0, -20^o C), whereas, a severe reduction in fatigue life is noted at 100 and 150^o C. Fatigue life of class 1 laminates decrease by as much as 3 orders of magnitude at 100^o C as compared to room temperature.
At a test temperature of 150^o C fatigue resistance is further degraded very severely. Fatigue strength at 10^6 cycles is decreased from 380 MPa at room temperature to 260 MPa at 150^{o}C. This severe degradation of fatigue strength at 150^o C is quite expected because this test temperature was well above the matrix glass transition temperature of 116^o C. Matrix material at this elevated temperature was notably disintegrated and was responsible for severely lowering the fatigue resistance of the composite.

Although unidirectional $[0]_8$ laminates exhibit better fatigue resistance than the angle plied $[0,0,45,-45]_s$, the cross ply laminates show a better ability to handle the influence of temperature than their unidirectional counterparts as can be seen form comparing figures 1 and 2. It is evident that in cross ply (class 2) laminates fatigue life is not lowered as severely as observed in the unidirectional (class 1) laminates. When compared to room temperature fatigue life at 100^o C for theses laminates is lowered by only a factor of 6 to 8 as against by 3 orders of magnitude observed in class 1 laminates.

4. GENRALIZED DAMAGE BEHAVIOR

The two main characteristics of WCFRP composites, which have a major influence on the manner in which fatigue damage occurs are, the in-homogeneity, and anisotropy of the composite laminates. In-homogeneity and anisotropy contributes greatly to fatigue damage localization process. Localized damage events like matrix cracking, fiber-matrix debonding, and localized ply separation act as damage initiators. However, after initiation, the damage growth is severely inhibited due to different properties and responses of adjacent plies or adjacent matrix phase. In fact, this constraint on damage growth forms the basis for a progressive localization and intensification of damage in a successively smaller volume of material as load cycling continues. This localization process is repeated throughout the laminates at different locations, which eventually merge to cause major delamination and final fracture.

Top

4.1 Optical Microscopy Observations

The first damage event that ensues very early during fatigue is the formation of Transverse Matrix Cracks (TMCs). Figure 3 represents an optical micrograph of the edge of a class 1 laminate, and displays such multiple TMCs formed in the matrix material present between the fiber bundles. These TMCs, which initiate mainly at the cross over points of weft (fiber bundles at 90^o to loading direction) and warp (fiber bundles at 0^o to the loading direction) fiber bundles, induce localized ply delamination. Figure 4 shows a typical transverse matrix crack, which has induced interply delamination at such cross over points. Figures 5a and 5b presents an optical view of the edge of a Class 1 specimen fatigued at room temperature and show ply delamination at 50 and 70% of fatigue life. In class 1 laminates this ply delamination remains localized at the specimen edges, and act as the initiator of the damage. The final failure in these laminates occurs mostly by the catastrophic fracture of warp fiber bundles. This observation is in agreement with the finding of [Khan et al, 1998].

In class 2 laminates, the initiation process is somewhat different due to the presence of angle plies. Initially Transverse Matrix Cracks (TMCs) appear through the weft of 0^o fiber bundle, which is at 90^o to the loading direction. These TMC travel inward from the edge of the composite and this process proceeds with cyclic loading similar to Class 1, creating ultimately a major edge delamination. The final failure occurs by severe delamination and fiber bundle fracture as discussed in the fractography section below. Test temperature was not observed to play any appreciable role in the formation of TMCs in both types of laminates. X-ray radiography however revealed (as discussed below) that the test temperature did have a significant influence on ply delamination characteristics of the composite

4.2 X-Ray Radiography Observation

Figures 6 and 7 show enhanced die X-ray radiographs of the composite laminates fatigued at various temperatures. Figure 6 represents the failure (a) at room temperature, (b) at -20^{o}C, and (c) at 0^o C, of class 1 laminates. As is evident from the radiographs, noticeable amount of edge ply delamination occurs at room temperature, whereas, at –20^{o}C and 0^{o}C, the failure occurs without discernible ply delamination. At all three temperatures the final failure has occurred predominantly by catastrophic fiber bundle fracture evidenced by the flat fracture planes. Figure 7 shows the x-ray radiographs of class 2 laminates fatigued at 0^{o}C, room temperature, and 100^{o}C, respectively. It is evident that in these laminates final fracture occurs mainly due to extensive delamination. At 100^{o}C the delamination between 0^o and 45^o plies is much severe than at room temperature. At 0^{o}C the amount of ply delamination further decreases, and the final fracture appears to be much flat, indicating that fiber bundle fracture is more dominant than delamination at 0^{o}C.

The results of these X-ray radiographs can be summarized as follows: the damage sequence in Class 1 is almost the same at all test temperatures. The primary matrix cracks are the initiators of fracture at all test temperatures. In class 2, the local debonding, which is actually a reason for delamination growth at cross over points, is significantly affected by temperature. At lower temperatures, the delamination growth is almost negligible and final fracture is very catastrophic by fracture of fibers in warp bundles. At higher temperatures, failure occurs after an extensive delamination growth has taken place.

4.3 Fractrographic Observations

As discussed above fatigue damage in the composite initiates by the formation of transverse matrix cracks, which due to the presence of higher stress concentration, mainly form at the cross over points between weft and warp fiber bundles and induce localized ply delamination. As the fatigue cycling continues ply delamination grows and cause weft fiber bundles to split and fracture setting the stage for final fracture which occurs either mainly by eventual fracture of warp fiber bundles (as in class 1) or by mainly extensive ply delamination (as in class 2) laminates.

Scanning electron fractography of the fracture surface of the fatigued specimen confirm the above sequence of fatigue damage. Figure 8 shows the fracture surface of a class 1 laminate fatigued at room temperature. This fractograph clearly show the transverse matrix cracking, ply delamination, and catastrophic fracture of warp fiber bundles. A higher magnification SEM fractograph in figure 9 shows the fracture of the matrix via transverse cracking, splitting and debonding of warp fiber bundles, and the fracture of individual fibers of the warp bundle in a class 1 laminate at room temperature.

Figure 10 shows a complete delaminated region between 0^{o} and 45^{o} plies in a class 2 CFRP specimen. The fracture can be observed to have occurred after extensive delamination. Similarly 45^{o} and -45^{o} fiber bundles can be seen separated due to substantial interfacial delamination due to shearing of the plies. It can be noticed that fractured fibers carry few matrix debris on the surface indicating fiber/matrix debonding before fracture.

The effect of temperature on the fatigue damage behavior can be summarized as follows. The two main items that experience the major influence of the temperature are the matrix material behavior and the fiber/matrix interfacial bonding. The change in matrix damage behavior with temperature is presented in Figures 11and 12. At room temperature matrix cracks in more or less flat brittle type of failure (Fig. 11) as compared to a much more ductile nature at 100^o C. Another enlarged view of ductile behavior of matrix at 100^o C is presented in Figure 12 where presence of large hackles clearly indicates that the matrix has indeed behaved in somewhat viscoelastic manner at 100^{o}C.

The fiber/matrix interfacial bonding is also a function of temperature. Figures 13-15 show fracture surface morphology of class 1 laminates fatigued at room temperature, 100^o C, and 150^o C, respectively. The small cusps on fracture surface in figure 13 show that a strong interfacial bonding existed between matrix and the fibers at room temperature. On the other hand, figures 14 and 15 reveal a weak fiber-matrix bonding at 100^{o}C and 150^{o}C. In fact at 150^{o}C, fibers seem to have completely debonded from matrix and tore off at final failure. Figure 15 in fact shows that almost a complete degradation (charring) of the matrix has occurred at 150^{o}C.

5. CONCLUSIONS

The findings of this study suggest a strong influence of temperature on the fatigue resistance and fatigue damage behavior of woven carbon fabric/epoxy composite laminates. Damage in these laminates occur by formation of transverse matrix cracks at cross over points early in life, followed by localized delamination, fiber matrix debonding. Final fracture in the class 1 unidirectional $[0]_8$ laminates occurs by catastrophic fracture of fibers of warp bundles. In the case of class 2 cross ply $[0,0,45,-45]_s$ extensive ply delamination is responsible for the final fracture. The unidirectional $[0]_8$ stacking sequence exhibits better resistance to fatigue loading than the cross ply $[0,0,45,-45]_s$ stacking sequence. However, substantially much more pronounced influence of temperature on the fatigue life of unidirectional (class 1) laminates is observed than the one noticed in cross ply (class 2) laminates. Substantial improvement in fatigue resistance is observed at temperatures above RT, whereas, it is severely degraded at temperatures above RT. It is suggested that this lowering of fatigue resistance results from the weakening between the fiber/matrix bonding at temperature above room temperature. A strong fiber/matrix bonding at temperatures below room temperature is responsible for the observed improvement in fatigue resistance of the WCFRP laminates.

ACKNOWLEDGEMENT

The authors wish to thankfully acknowledge King Fahd University of Petroleum & Minerals, Dhahran, Saudi Arabia for its support of this research work.

REFERENCES

1. Todoroki, A., Kobayashi, H., and Lee, J. G., 1994, "Image Analysis of Delamination Cracks in Carbon Fiber Composites by Scanning Acoustic Microscopy" Composites science and technology, Vol 52, pp 551-559.
2. Kim, S.T., and Lee, Y., 1997, "Characteristics of damage and fracture process of carbon fiber reinforced plastic under loading-unloading test by using AE method" Material Science and Engineering, A234-236, pp 322-326.
3. Takemura, K., and Fuji, T., 1994, "Fatigue Damage And Fracture Of Carbon Fabric/Epoxy Composites Under Tension-Tension Loading" JSME international journal, series A, V 37, n 4, pp 472-480
4. Smith R. A. and Clarke, B., 1994, "Ultrasonic C-Scan Determination of Ply Stacking Sequence in Carbon Fiber Composites" Insight, v 36, n 10, pp 741-747.
5. Dillon G. and Buggy M., 1995 "Damage Development during Flexural Fatigue of Carbon Fiber Reinforced Peek" Composites, V 26, pp 355-370.
6. Takeda, N., Oghira, S., Suzuki, S., and Kobayashi, A., 1998 " Evaluation of Microscopic Deformation in CFRP Laminates With Delamination by Micro Grid Methods" Journal of composite materials, V 32, n 1, pp 83-100.
7. Gilchrist M.D., Sevenson, N., and Shishoo, R., 1998, "Fracture and fatigue performance of textile commingled yarn composites" Journal of Materials Science, V 33, pp 4049-4058.
8. Khan, Z., Al-Sulaiman, F.S., and Farooqi, J.K., 1998, “Fatigue Damage Characterization in Plain weave Carbon-carbon Fabric Reinforced Plastic Composites” Journal of Reinforced Plastics and Composites, V 17, No. 15, pp 1320-1337.
9. Miyano, Y., McMurry, M.K., Enyama, J., Nakada, M., 1994, "Loading Rate and Temperature Dependence on Flexural Fatigue Behavior of a Satin Woven CFRP Laminate" Journal of Composite Materials, V 2, n 13, pp 1250-1260.
10. Miyano, Y., Kanemitsu, M., Kunio, T., Kuhn, H., 1986, "Role of matrix resin on fracture strengths of unidirectional CFRP" Journal of composite materials, V 20, pp 520-538.
11. Miyano,Y., Nakada, M., McMurry, M.K., Muki, R., 1997, “Prediction of Flexural Fatigue Strength of CFRP Composite Under Arbitrary Frequency, Stress ratio and Temperature” Journal of Composite Materials, 31, No.6.
12. Matsuhisa, Y.; King, J.E., 1993, “Effects of Temperature on Monotonic and Fatigue Properties of Carbon Fiber Epoxy Cross Ply Laminates” Journal de Physique 3.
13. Nakamura, M., Suzuki, H., Haraguchi, T., Watanabe, Y., 1998, "Influence of environmental temperature on fatigue reliability at elevated temperature for carbon fiber reinforced PEEK (on the growth mechanism from mesocracks to macrocrack)" JSME International Journal, Part A, V 63, No 606, pp 213-219.

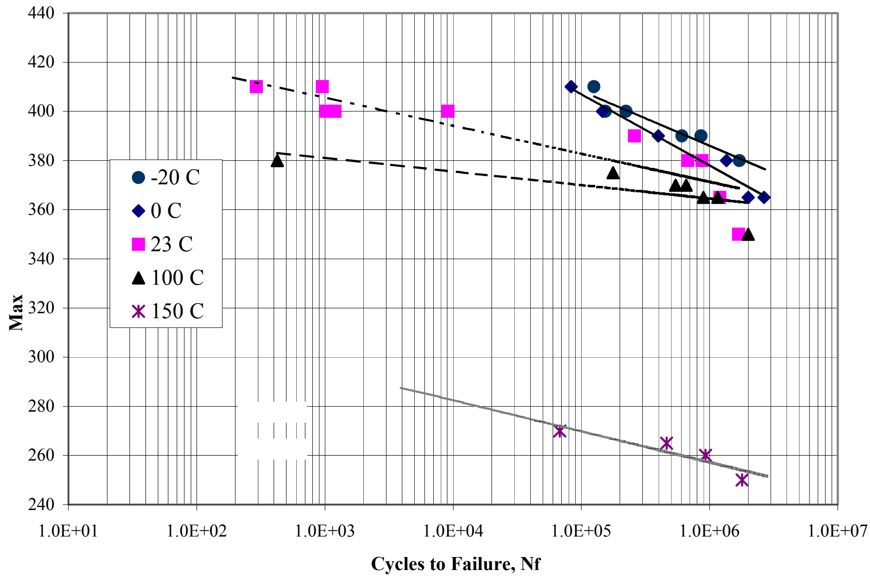

Fig. 1 Fatigue test results (SN curves) for class 1 $[0]_8$ laminates at various test temperatures

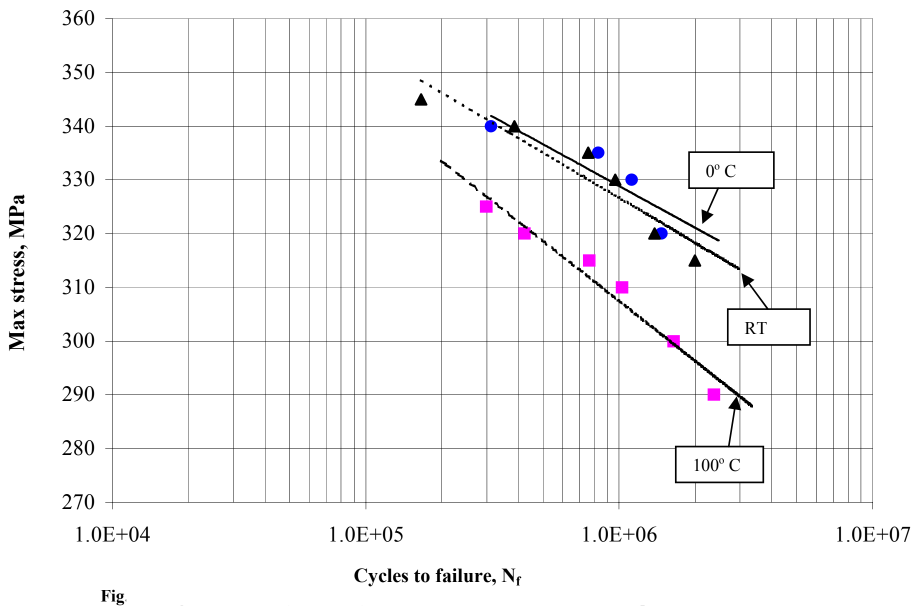

Fig. 2 Fatigue test results (SN curves) for class 2 $[0,0,45,-45]_s$ laminates at various test Temperatures.

Top

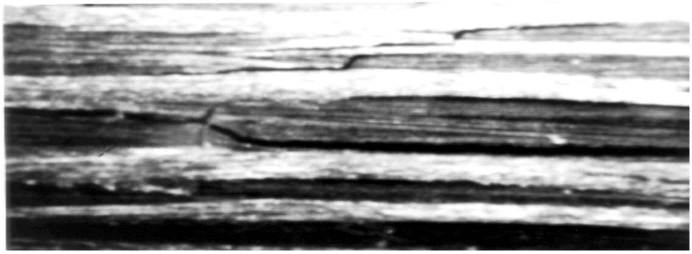

Fig. 3. Photomicrograph showing multiple cracks in off-axis plies and delamination in a Class $1[0]_8$ laminate. 40x

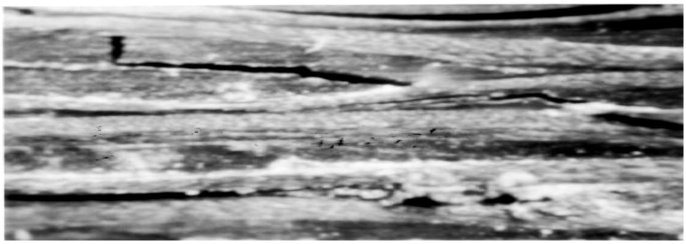

Fig. 4 Photomicrograph showing matrix crack and delamination in a Class $1[0]_8$ laminate. 40x

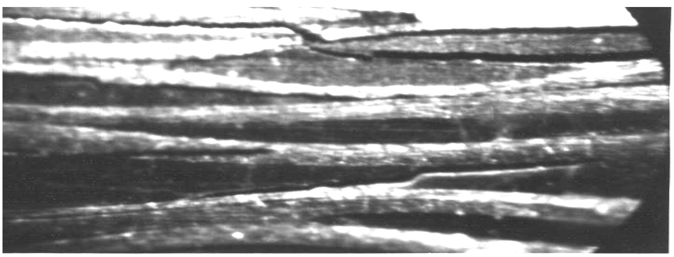

Fig. 5 (a) Photomicrograph showing matrix cracks and delamination at 50% of fatigue life for a class 1 laminate. 40x

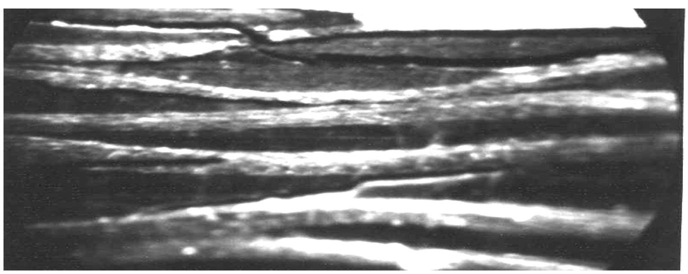

Fig 5 (b) Photomicrograph showing matrix cracks and delamination at 70% of fatigue life for the laminate shown in 5(a). 40x

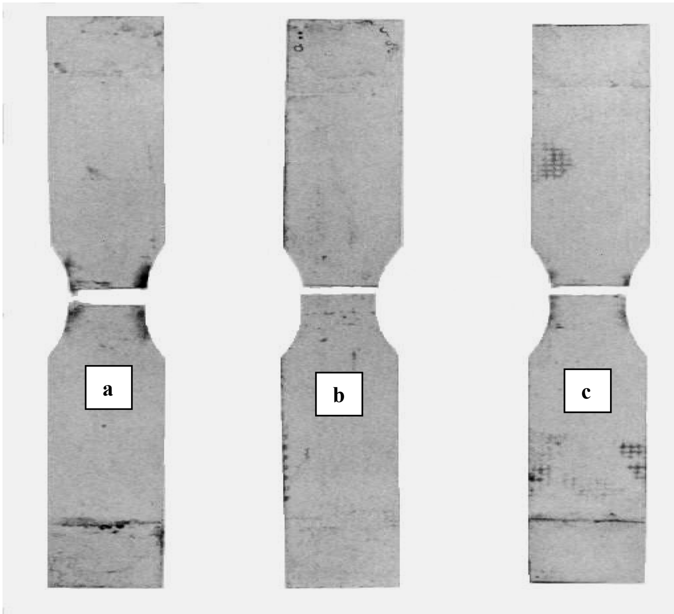

Fig. 6 X-ray radiograph showing failure at (a) room temperature, (b) -20^{o}C and (c) 0^{o}Cfor Class 1 laminates.

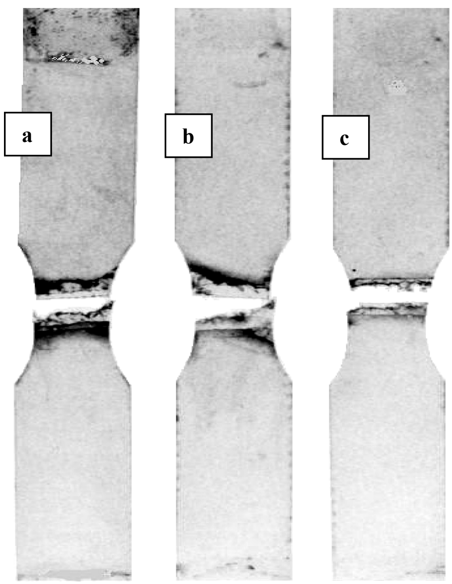

Fig. 7 X-ray radiograph showing delamination in class 2 laminate at (a) 100^{o} C, (b) RT (c) 0^{o} C.

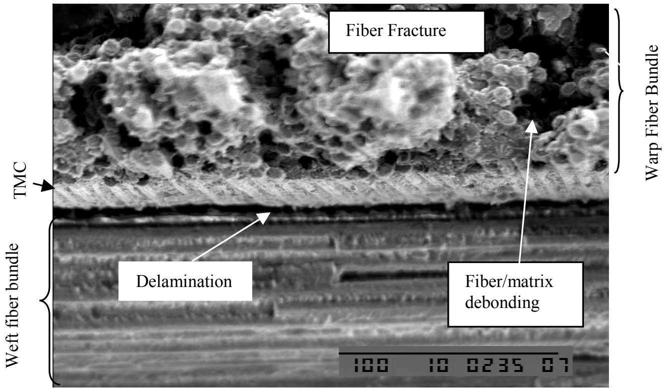

Fig. 8 SEM fractograph showing damage events in a Class 1 $[0]_8$ laminate.

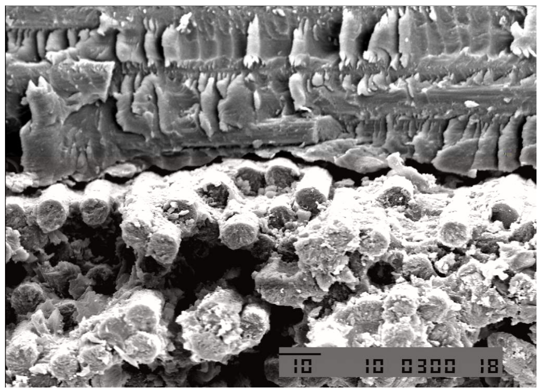

Fig. 9 SEM fractograph showing matrix cracking and warp fiber splitting and bundle fiber fracture.

Fig. 10 SEM fractograph showing fiber bundle fracture and delamination in class 2 laminate.

Top

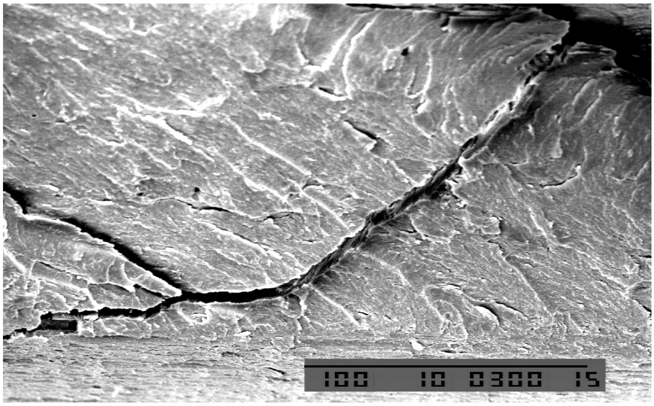

Fig. 11 SEM fractograph showing matrix cracking at Room temperature in a Class 1 $[0]_8$ laminate.

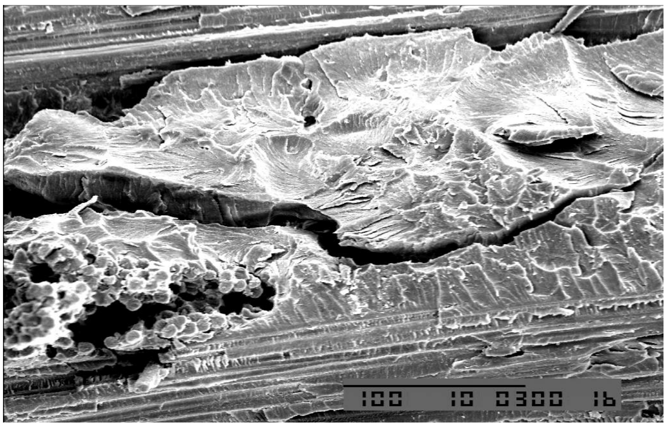

Fig. 12 SEM Micrograph showing matrix cracking at 100°C in a Class 1 $[0]_8$ laminate.

Top

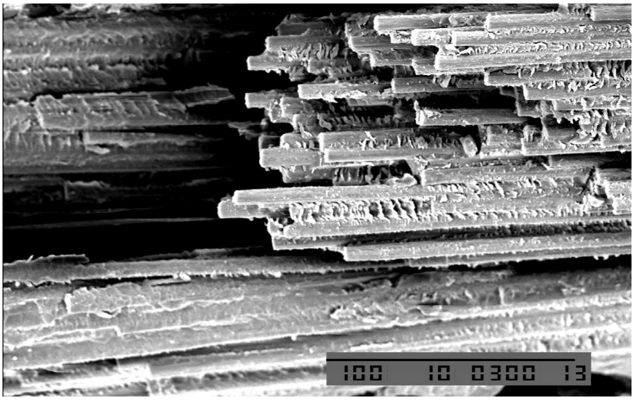

Fig. 13 SEM fractograph showing the effect of temperature on fiber/matrix bonding at 24^{o}C in a Class 1 laminate.

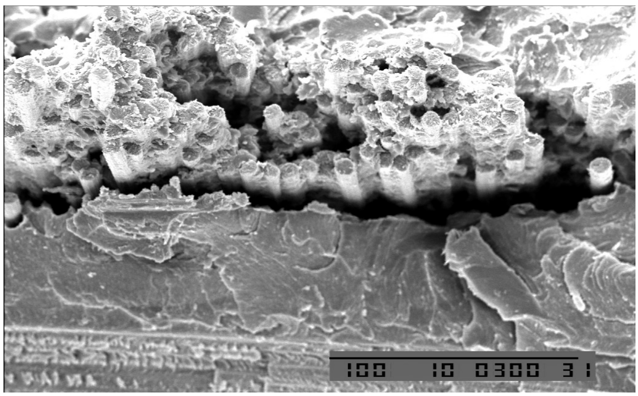

Fig. 14 SEM fractograph showing the effect of temperature on fiber/matrix bonding at 100^{o}C in a Class 1 laminate.

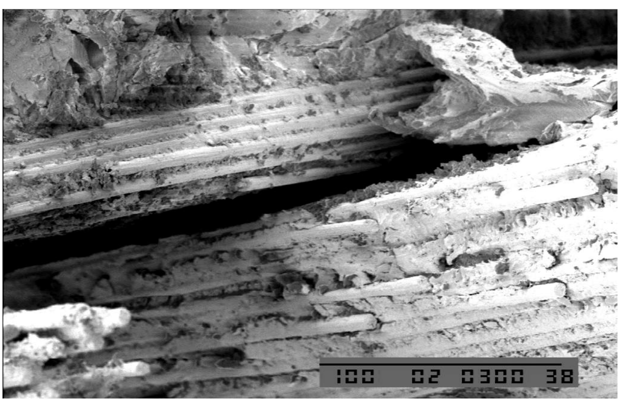

Fig. 15 SEM fractograph showing the disintegration of matrix at 150^{o} C in class 1 laminate.

Top